13 Superconductivity in 4-Angstrom Carbon Nanotubes

Ping Sheng, Z. K. Tang, Lingyun Zhang, Ning Wang, Xixiang Zhang, G. H. Wen, G. D. Li, Jiannong Wang and C. T. Chan
Department of Physics and Institute of Nano Science and Technology, Hong Kong University of Science and Technology, Clear Water Bay, Hong Kong, China

ABSTRACT

We report the observation of intrinsic one-dimensional (ID) superconductivity in 0.4 nm-sized single-walled carbon nanotubes (SWNTs), fabricated by pyrolyzing tripropylamine in the channels of zeolite $AlPO_4$-5 single crystals. These ultra-small SWNTs are highly aligned, uniform in size, and isolated from each other. They constitute an almost ideal 1D conducting system. The superconductivity of these ultra-small exhibits one-dimensional fluctuations, and displays smooth temperature variations with a mean-field superconducting transition temperature of 15 K. The data are consistent with the manifestations of a 1D BCS (phonon-mediated) superconductor.

1. INTRODUCTION

Since the discovery of carbon nanotubes in 1991 (Iijima, 1991), researches have alluded to the possibility of their use as current carrying devices. The electronic properties of a single-walled carbon nanotube (SWNT) are known to be solely determined by its geometric structure. It was shown within the band-folding scheme that only the zero-helicity armchair tubes have zero electronic band gap, the others being small gap semiconductors or insulators depending on their radius and chirality (Blasé, 1994; Dresselhaus, 1996; Saito, 1998). In very small SWNTs, however, the presence of σ^*-π^* hybridization introduced by the strong curvature effect (Blasé, 1994) can lead to novel electronic properties departing from the prediction of the band-folding theory (Blasé, 1994; Zhao, 2001). The increased curvature also opens new electron-phonon scattering channels that enhance the electron-phonon coupling and make superconductivity likely (Benedict, 1995). Experimentally, superconductivity has recently been observed in ropes of SWNTs (1.4 nm diameter) at temperature below 0.55 K (Kociak, 2001), and in 0.4 nm sized SWNTs at a mean-field superconducting temperature as high as 15 K (Tang, 2001).

In this paper, we report the observation of 1D superconductivity in 0.4 nm SWNTs accommodated in the channels of a zeolite $AlPO_4$-5 (AFI) single crystal (Tang, 1989; Wang, 2000). These nanotubes have been observed directly by transmission electron microscopy (Wang, 2000; Wang, 2001), and indirectly by X-ray diffuse scattering (Launois, 2000) as well as by micro-Raman

measurements of the nanotube breathing mode (Sun, 1999a; Sun, 1999b). The data consistently indicate a nanotube diameter of 0.4 nm, probably at or close to the theoretical limit. Because the single-walled nanotubes (SWNTs) are formed inside the ordered channels of AFI, they are highly aligned and uniform in size; and because the SWNTs are isolated from each other, they constitute an almost ideal 1D system. The measured magnetic and transport properties revealed that at temperatures below 20 K, these ultra-small SWNTs exhibit superconducting behavior manifest as an anisotropic Meissner effect, with a superconducting gap and fluctuation supercurrent. The measured superconducting characteristics display smooth temperature variations owing to one-dimensional fluctuations, with a mean-field superconducting transition temperature of 15 K. Statistical mechanic calculations based on the Ginzburg-Landau free energy functional yield predictions that are in excellent agreement with the experiments.

2. SAMPLE PREPARATION AND MEASUREMENTS

The SWNTs were produced in the channels of AFI single crystals by pyrolysis of tripropylamine (TPA) hydrocarbon molecules contained in the zeolite channels, under a vacuum of 10^{-3} Torr and a temperature of 500-600 °C (Tang, 1998). The nanotubes-containing AFI crystals behave as good polarizers with high absorption for light polarized parallel to the channel direction ($E//c$) and transparent for light polarized perpendicular to the c-axis ($E\perp c$), characteristic of one-

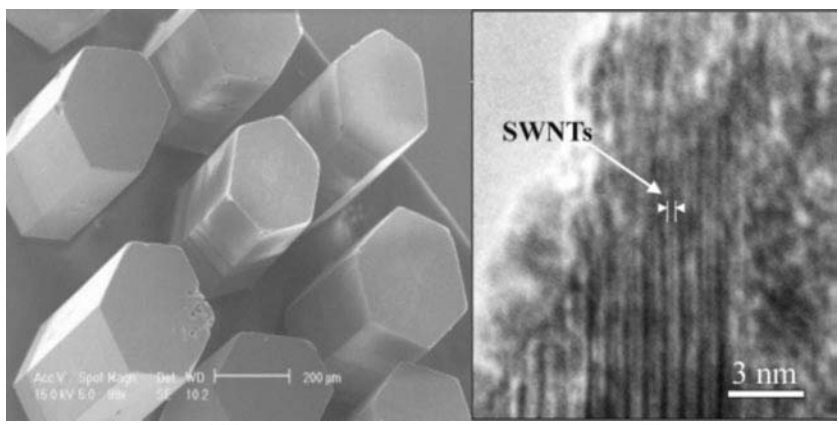

Figure 1 (a) A SEM image of the nanotubes-containing AFI single crystals. The nanotubes are too small to be visible on this scale. (b) A TEM image of a nanotubes-containing AFI crystal, broken on one side to reveal the channel structure of the AFI crystal and the nanotubes lying inside the channels.

dimensional anisotropic conductors. Figure 1(a) shows the scanning-electron-microscope (SEM) image of the nanotubes-containing AFI single crystals. The crystals have a beautiful hexagonal columnar shape with a typical dimension

of 100×100×500 μm^3. Figure 1(b) is a high-resolution transmission electron microscope image of the SWNTs lying inside the AFI zeolite channels. For TEM images of free standing SWNTs after the zeolite matrix has been dissolved, please refer the earlier works (Wang, 2000; Wang, 2001). To measure the electrical transport properties, a single hexagonal column was first cut into a square cross sectional shape and fixed tightly with thin glass plates on four sides. The sample was then polished into a thin slab with a thickness of a few micrometers. Electrical contacts were made by evaporating a thin layer of gold on the two ends of the nanotubes-containing AFI crystal. The conductance of the nanotubes was measured in the two-probe configuration at temperatures ranging from 300 K to 0.3 K. Temperature-dependent magnetic susceptibility was measured by using a Quantum Design superconducting quantum interference device magnetometer (MPMS-5S) equipped with a 5 Tesla magnet.

3. RESULTS AND DISCUSSION

3.1. One Dimensional Hopping Conductivity

Figure 2 is the current-voltage curves of the ultra-small SWNTs measured at different temperatures. At room temperature the conductivity of the SWNTs is on the order of 10^{-1} $\Omega^{-1}cm^{-1}$, lower than the conductivity reported for the metallic single-wall carbon nanotubes with larger diameters (Ebbesen, 1996; Thess, 1996;

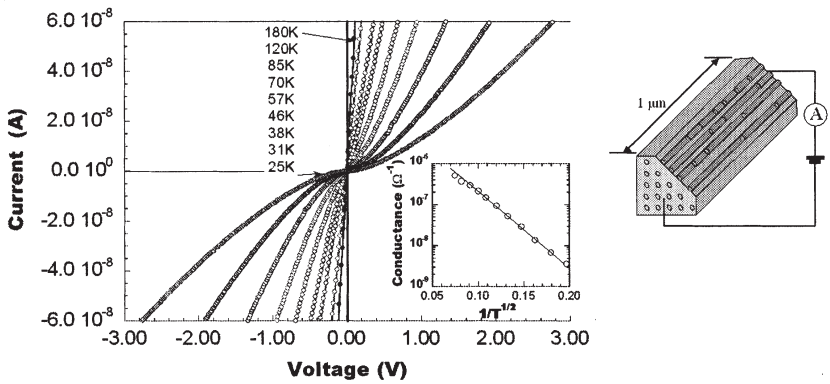

Figure 2 Current-voltage curves measured for the 0.4 nm-sized SWNTs at different temperatures. Inset: the conductance measured at near zero bias voltage and plotted in a semi-logarithm as a function of $1/T^{1/2}$. The measurement configuration is also shown in the right.

Kasumov, 1996). The temperature-dependent conductance measured near zero-bias voltage is shown in the inset. It is seen that the logarithm of conductance decreases linearly as $1/T^{1/2}$, typical of 1D hopping conduction (Sheng, 1995). This is due to the fact that each SWNT is most likely to have defects along its length, leading to localized electronic states. Thus electrical conduction is by hopping, i.e., thermal activation plus tunneling, from one localized site to another. Exp $(-1/T^{1/2})$ is the signature of hopping conduction in 1D systems. The inset to Fig. 3 shows the *I-V* curves measured at temperatures lower than 20 K. As seen, a gap

seems to open at the Fermi level at temperatures below 15 K. This is evidenced by the disappearance of charge carriers at low voltages. For every temperature, there exists a clear voltage threshold above which the charge carriers appear again. The value of the threshold, which may be estimated by extrapolating from the asymptote back to the horizontal axis, increases with decreasing temperature. The temperature variation of the threshold voltage is summarized in Fig. 3. This behavior is reproducible not only on the same sample, but also on different samples. In light of the experimental data on the Meissner effect, obtained later chronologically, this gap-opening is interpreted to be indicative of the transition from the normal to the superconducting phase, accompanied by the opening of the superconducting gap. Because of the imperfection in the nanotubes (as seen in the 1D hopping conduction), a series of superconducting pieces of the nanotubes are

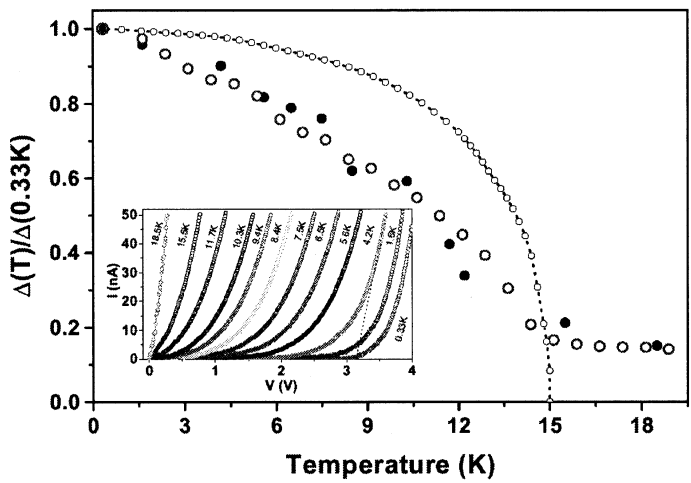

Figure 3 Inset: Current-voltage curves at temperatures lower than 20 K. For each temperature below 15 K, there exists a threshold in the *I-V* curve. The temperature dependence of the threshold voltage is shown by open circles. Solid symbols denote theory. For comparison, the BCS gap is also shown as the circle-dashed curve.

separated by potential barriers. Thus, the I-V curves measure only the normal current, as the potential barriers would destroy the phase coherence required for the observation of the supercurrent. Thus the threshold in each of the I-V curves is a measure of the superconducting gap, in the manner of I. Giaever's early tunneling experiments (Giaever, 1960).

3.2. Anisotropic Meissner Effect

To confirm the superconductivity at temperatures below 20 K, we measured magnetization properties for the SWNTs as a function of temperature and magnetic field. Two samples were measured. Sample A, used for background deduction, consists of columnar zeolite crystallites with empty channels, about 300 μm long and 100 μm in diameter. Sample B is composed of similar crystallites but with nanotubes formed inside their channels. For both samples, the

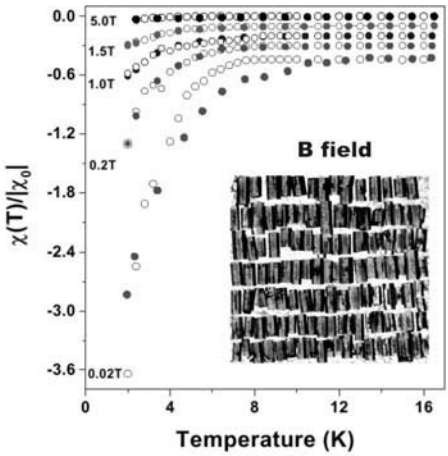

Figure 4 Normalized magnetic susceptibility of the SWNTs plotted as a function of temperature for five values of the magnetic field. Experimental values (filled circles) and theoretical predictions for the fluctuation super-current (open circles) are shown. The inset shows the aligned nanotube samples and the direction of applied magnetic field.

c axes of the crystallites were aligned by hand to form a parallel array and fixed. It is estimated that there is a maximum error of ±10° in the alignment. All samples were dried and weighed. The magnetization was measured as a function of temperature while warming from 1.8 to 50 K. At each temperature, the magnetization was measured after the temperature was stabilized for 60 seconds. The measured magnetization is anisotropic with respect to the field orientation. After a simple deduction of the pure zeolite crystallite contribution and normalizing to the nanotube volume, the temperature dependence of the SWNTs' magnetic susceptibility is shown in Fig. 4, for five values of applied field perpendicular to the *c* axes. For the perpendicular field case, a strongly temperature-dependent diamagnetism is seen below 10 K, at 0.02- or 0.2-T applied field. The magnitude of the susceptibility decreases monotonically with increasing field and is very small at 5 T. The result is in quantitative agreement with the Meissner effect of 1D fluctuation superconductivity (Tang, 2001), described briefly below. The susceptibility of the parallel field case is one order of magnitude less, within the error caused by the crystallites' misalignment and consistent with the observation that there is no Meissner effect under a parallel field for 1D systems. Thus the nanotube susceptibility is anisotropic. The Meissner effect associated with 1D superconductivity differs substantially from the conventional behavior of an abrupt susceptibility jump at superconducting-transition temperature T_c. Here, the dominance of 1D fluctuations means that the critical phenomenon around T_c is replaced by smooth temperature and magnetic-field variations.

3.3. One Dimensional Fluctuation Supercurrent

In order to verify the consistency of the physical picture that superconductivity exists in segments along the nanotubes, it is necessary to observe the supercurrent within each of the segments. However, in order to do that it is necessary to fabricate thin samples so as to ensure that there are no imperfections (potential barriers) within the length of the SWNTs. A rough estimate of the sample thickness required is provided by the measured voltage threshold at low temperatures (about 4 volts) and the relevant sample thickness (100 microns). Since a mean field T_c of 15 K would imply a superconducting gap of ~4 meV, there should be ~1000 potential barriers over 100 microns. That means an average superconducting segment of ~100 nanometers. Experimentally, a sample thickness of 50 nm is achieved by argon ion milling both sides of the sample. Such a thin foil is translucent as observed by SEM (shown in the inset of Fig. 5). After etching (with HCl) and cleaning (with distilled water) of the foil, Pt electrodes were made on both sides of the foil by FIB deposition. The size and location of the Pt electrodes were precisely controlled by FIB, ensuring good contact between the electrodes and the ends of SWNTs. In Fig. 5 the measured conductance ΔG (measured at 1V, or an electric field $\approx 2\times10^5$ V/cm) is plotted as a function of temperature. The observed temperature dependence is opposite to the thick sample. Moreover, the conductance of the sample exhibits a diverging behavior, very different from the usual metallic behavior of saturation at low temperatures. As seen below, such behavior is characteristic of fluctuation supercurrent in 1D, consistent with both the magnetic Meissner effect as well as the appearance of the gap.

4. THEORY

To explain the observed Meissner effect, the appearance of the gap, and the supercurrent, it is necessary to note that in contrast to 3D systems where fluctuations may be regarded as a perturbation, in a 1D system fluctuations can be

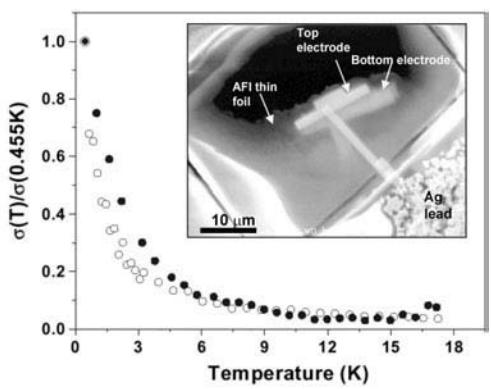

Figure 5 The normalized conductivity plotted as a function of temperature for the thin sample. Experimental values (filled circles) and theoretical predictions for the fluctuation super-current (open circles) are shown. The inset shows the SEM image of the sample after thinning by argon milling.

so dominant as to alter its thermodynamic properties (Mermin, 1966). Here, what that means is that while locally the system is superconducting at temperatures below T_c = 15 K, it is characteristic of 1D systems that the divergening long-wavelength fluctuation amplitudes, when considered together with the density of states, means that macroscopically, the superconducting transition can only be achieved at T = 0 K. Between $T = T_c$ and T = 0 the superconductivity is not totally destroyed but can manifest superconducting behavior strongly modified by the fluctuation effects. To calculate such behavior statistically requires the numerical evaluation of functional integrals. That is, the partition function of the system may be written as

$$Z = \int D[\psi(x)] \exp\{-\beta F_{GL}[\psi(x)]\}, \qquad (1)$$

where $\beta = 1/kT$, with k the Boltzmann constant, and $F_{GL}[\psi(x)]$ the Ginzburg-Landau (GL) free energy functional (Ginzburg, 1950), containing four phenomenological parameters. $D[\psi(x)]$ means functional integration over all possible fluctuation configurations as represented by a spatially dependent complex wavefunction $\psi(x)$, whose magnitude is proportional to the superconducting gap. The total free energy of the system is $F = -kT \ \ell nZ$. For a perpendicular applied magnetic field $\vec{B}$, $\vec{A} = Bx\ \hat{j}$, with $\hat{j}$ the unit vector along the y direction. The magnetic susceptibility is given by $\chi = -\partial^2 F / \partial B^2$. Details of the calculations are given in (Tang, 2001). It suffices to mention that the solid symbols in Fig. 4 are theory predictions obtained with four fitting parameters. However, once these parameter values were fixed, the solid symbols in Fig. 3 and Fig. 5 were obtained with no further adjustable parameters. The good agreement between theory and experiment show that all the three phenomena can be consistently explained on the basis of a single theoretical framework. In the case of the fluctuation supercurrent, the sample at $T \le T_c$ cannot be at zero resistance (even without potential barriers) because at any given instant there is always some probability that fluctuations would locally drive the superconducting state to the normal state. In a 1D system, any normal segment is in series with the rest of the sample, and hence there is always a finite resistance at finite temperatures. Because such a probability decreases with temperature, the fluctuation supercurrent, and hence the conductance, increases. Zero resistance is reached only at T = 0 K.

In summary, we have fabricated mono-sized, 4 Å SWNTs in the channels of zeolite single crystals. Investigation of the magnetic and transport properties of the SWNTs revealed superconducting behavior manifest as an anisotropic Meissner effect, with a superconducting gap and fluctuation supercurrent. The measured superconducting characteristics can be consistently explained by a unified theoretical framework based on the Ginzburg-Landau free energy functional.

ACKNOWLEDGEMENT

We thank K. Y. Lai for his technical assistance on the FIB system, and T. K. Ng, P. Yu, and L. Chang for helpful comments. This work is partially supported by RGC grants of HKUST6152/99P, DAG00/01.SC27, SAE95/96.SC01, and HIA98199.SC01.

REFERENCES

Benedict L. X., Crespi V. H., Louie S. G. and Cohen M. L., 1995, Static conductivity and superconductivity of carbon nanotubes: relations between tubes and sheets, *Physics Review B*, **52**, pp. 14935-14940.

Blase X., Benedict L. X., Shirley E. L. and Louie S. G., 1994, Hybridization effects and metallicity in radius carbon nanotubes, *Physics Review Letters*, **72**, pp. 1878-1881.

Dresselhaus M. S., Dresselhaus G. and Eklund P. C., 1996, *Science of Fullerenes and Carbon Nanotubes*, (San Diego: Academic).

Ebbesen T. W., Lezec H. J., Hiura H., Bennet J. W., Ghaemi H. F. and Thio T., 1996, Electrical conductivity of individual carbon nanotubes, *Nature*, **382**, pp. 54-56.

Giaever I., 1960, *Physical Review Letters*, **5**, pp. 147-150.

Ginzburg V. L. and Landau L. D., 1950, *Zh. Eksp. Teor. Fiz.*, **20**, pp. 1064.

Iijima S., 1991, Helical microtubules of graphitic carbon, *Nature*, **354**, pp. 56-58.

Kasumov A. Y., Khodos I. I., Ajayan, P. M. and Colliex C., 1996, Electrical resistance of a single carbon nanotube, *Europhysics Letters*, **34**, pp. 429-434.

Kociak M., Kasumov A. Y., Gueron S., Reulet B., Khodos I. I., Gorbatov Y. B., Volkov V. T., Vaccarini L. and Bouchiat H., 2001, Superconducivity in ropes of single-walled carbon nanotubes, *Physical Review Letters*, **86**, pp. 2416-2419.

Launois P., Moret R., Le Bolloc'h D., Albouy P. A., Tang Z. K., Li G. and Chen J., 2000, Carbon nanotubes synthesised in channels of $AlPO_4$-5 single crystals: first X-ray scattering investigations, *Solid State Communications*, **116**, pp. 99-103.

Li Z. M., Tang Z. K., Liu H. J., Wang N., Chan C. T., Saito R., Okada S., Li G. D. and Chen J. S., 2001, Polarized absorption spectra of single-walled 0.4 nm carbon nanotubes aligned in channels of $AlPO_4$-5 single crystal, *Physical Review Letters*, **87**, pp. 127401-127404.

Mermin N. D. and Wagner H., 1966, *Physics Review Letters*, **17**, pp. 1133-1136.

Saito R., Dresselhaus G. and Dresselhaus M. S., 1998, *Physical Properties of Carbon Nanotubes* (London: Imperial College Press).

Sheng P., 1995, *Introduction to Wave Scattering, Localization, and Mesoscopic Phenomena*, (Academic Press), pp. 293-298.

Tang Z. K., Sun H. D., Wang J., Chen J. and Li G., 1998, Mono-sized Single-wall Carbon Nanotubes Formed in the Channels of $AlPO_4$-5 Single Crystal, *Applied Physics Letters*, **73**, pp. 2287-2289.

Tang Z. K., Zhang L. Y., Wang N., Zhang X. X., Wen G. H., Li G. D., Wang J. N., Chan C. T. and Sheng P., 2001, Superconductivity in 0.4nm diameter single walled carbon nanotubes, *Science*, **292**, pp. 2462-2465.

Thess A., Lee R., Nikolaev P., Dai H., Petit P., Robert J., Xu C. H., Lee Y. H., Kim S. G., Rinzler A. G., Colbert D. T., Scuseria G. E., Tombnek D., Fischer J. E. and Smalley R. E., 1996, Crystalline ropes of metallic carbon nanotubes, *Science*, **273**, pp. 483-486.

Wang N., Tang Z. K., Li G. D. and Chen J. S., 2000, Single-walled 4 angstrom carbon nanotube arrays, *Nature*, **408**, pp. 50-51.

Wang N., Li G. D. and Tang Z. K., 2001, Mono-sized single-walled 4 Å carbon nanotubes, *Chemical Physics Letters*, **339**, pp. 47-52.